Nested PARAFAC Tensor-based channel estimation method for double RIS-aided MIMO communication systems

Sepideh Gherekhloo[⋆], *Khaled Ardah*[‡], *André L. F. de Almeida*[†], *Marjan Maleki* [⋆], *and Martin Haardt*[⋆]
[⋆] Communications Research Laboratory (CRL), TU Ilmenau, Ilmenau, Germany
[‡] Lenovo (Deutschland) GmbH
[†] Wireless Telecommunications Research Group, Federal University of Ceará, Fortaleza, Brazil

***Abstract*—In this paper, we consider a double-RIS (D-RIS) aided MIMO system, where one RIS is deployed closer to the transmitter and another is placed closer to the receiver. We show that the received signals in flat-fading D-RIS aided MIMO systems can be represented as a 4-way tensor satisfying a nested PARAFAC decomposition model. Exploiting such a structure, a closed-form channel estimation method is proposed, where two out of three channels are estimated in parallel using the low-complexity Khatri-Rao factorization technique. Furthermore, we propose an alternating least squares (ALS)-based channel estimation method with an efficient initialization. The simulation results show that both proposed methods have a comparable performance as long as the identifiability conditions of the Khatri-Rao factorization are satisfied. The proposed ALS-based method can achieve a satisfactory performance with less training overhead. Moreover, the proposed ALS-based method performance can further be improved by using the Khatri-Rao factorization as an initialization.**

***Index Terms*—Double RIS, nested PARAFAC decomposition, Khatri-Rao Factorization, channel estimation.**

I. Introduction

Recently, reconfigurable intelligent surfaces (RISs) have been proposed as one of the key technologies to achieve smart radio environments. An RIS is a 2D surface equipped with a large number of tunable units that can be realized using, e.g., inexpensive antennas or metamaterials and controlled in real-time to influence the communication channels without generating its own signals [1]. Therefore, RISs have a great potential for improving the efficiency, the communication range, and the capacity of future wireless communication systems.

Most of the prior work, e.g., as in [2]–[6], [8], [9], considered single RIS-aided (S-RIS) systems, where a transmitter communicates with one receiver, or more, via a single RIS-aided channel. In such scenarios, it is shown that the S-RIS should be either deployed closer to the transmitter or closer to the receiver to achieve the best performance gain [7]. On the other hand, in many application scenarios, the transmitter might need a multi-RIS-aided channel to achieve a successful communication with the receiver. Among the multi-RIS-aided systems, the double-RIS (D-RIS)-aided ones have started to receive more attention, with the main focus on the RIS reflection design under the assumption of perfect channel knowledge as in [10], [11]. In [11], the passive beamforming gain of a D-RIS-aided systems, where one RIS is deployed closer to the transmitter and another is placed closer to the receiver, is compared to S-RIS-aided systems by exploiting the cooperative beamforming over inter-RIS channels. It is shown that D-RIS-aided systems can achieve a beamforming gain of $\mathcal{O}(N^4)$ as compared to $\mathcal{O}(N^2)$ with S-RIS-aided systems, where N is the total number of reflecting elements in the system.

On the other hand, channel estimation in D-RIS-aided systems is more problematic, since the cascaded (effective) channel contains three parts as compared to two in S-RIS-aided systems [11]–[14]. In [12] and [13], channel estimation procedure in the D-RIS-aided system were proposed for SISO and MISO systems, respectively. In [14], we have proposed an alternating least squares (ALS)-based channel estimation method by exploiting the Tucker2 tensor structure of the received signals. We have shown that by carefully distributing the N reflecting elements between two RISs in D-RIS systems, more accurate channel estimation with less training overhead can be achieved compared to S-RIS aided systems. To the best of our knowledge, our previous work [14] is the only work on channel estimation considering D-RIS-aided MIMO systems.

In this paper, and different from our previous work [14], we assume that the training overhead assigned to each RIS in D-RIS-aided MIMO systems can be adjusted separately. Consequently, we show that the received signals in flat-fading D-RIS aided MIMO systems can be represented as a 4-way tensor that satisfies a nested PARAFAC decomposition model [18], [21]. Exploiting such a structure, we propose a non-iterative three-step channel estimation method, where one of the three channel matrices in each step can be determined in closed-form using a low-complexity least squares Khatri-Rao Factorization (KRF) technique [19]. To enhance the channel estimation accuracy, we further propose an ALS-based channel estimation method where we estimate one channel matrix assuming that the other two are fixed. ALS has more relaxed

The authors gratefully acknowledge the support of the German Research Foundation (DFG) under grant no. HA 2239/14-1 (AdAMMM), grant no. ZH 640/2-1 (AdAMMM) and CAPES/PROBRAL Proc. 88887.144009/2017-00, CAPES/PRINT Proc. 88887.311965/2018-00.

constraints on the training overhead than the closed-form KRF method. Here, and different from our previous work [14], we propose to initialize two channel matrices using the closed-form KRF-based method. Using computer simulations, we show that the newly proposed ALS method with KRF-based initialization does not only have a faster convergence rate, but also has a better estimation accuracy as compared to the ALS-based method with random initializations proposed in [14]. Moreover, we show that both proposed methods have a comparable estimation accuracy if the identifiability constraints of the closed-form KRF method are satisfied. However, if less training overhead is used, then the ALS-based method outperforms the closed-form KRF-based method with less training overhead. Last but not least, both proposed channel estimation methods can be extended to a multi-user scenarios, where the channel estimation can be performed separately for each user with orthogonal training sequences in the time, frequency, and/or space domain without any multi-user interference. In the case of non-orthogonal pilot sequences, the block PARATUCK model can be used [15], where the associated factor matrices are block matrices. The number of matrix blocks is equal to the number of users. The complexity of the receiver would be higher in this case, since we estimate the channels of all users simultaneously.

Notation: The conjugate, the transpose, the conjugate transpose (Hermitian), the Moore–Penrose inverse, the Kronecker product, and the Khatri-Rao product are denoted as $\boldsymbol{A}^*$, $\boldsymbol{A}^\mathsf{T}$, $\mathbf{A}^\mathsf{H}$, $\mathbf{A}^+$, $\otimes$, and $\diamond$, respectively. Moreover, diag$\{\mathbf{a}\}$ forms a diagonal matrix $\mathbf{A}$ by putting the entries of the input vector $\mathbf{a}$ in its main diagonal, vec$\{\mathbf{A}\}$ forms a vector by staking the columns of $\mathbf{A}$ over each other, unvec$\{\mathbf{A}\}$ is the inverse of the vec operator, and the n-mode product of a tensor $\boldsymbol{\mathcal{A}} \in \mathbb{C}^{I_1 \times I_2 \times \ldots, \times I_N}$ with a matrix $\mathbf{B} \in \mathbb{C}^{J \times I_n}$ is denoted as $\boldsymbol{\mathcal{A}} \times_n \mathbf{B}$. Moreover, the following property is used: $\text{vec}\{\mathbf{ABC}\} = (\mathbf{C}^\mathsf{T} \otimes \mathbf{A})\text{vec}\{\mathbf{B}\}$.

II. System model

We consider a D-RIS aided MIMO communication system, where a transmitter equipped with M_{Tx} antenna elements is communicating with a receiver having M_{Rx} antennas via a D-RIS aided channel[1]. As depicted in Fig. 1, RIS 1 is assumed to be placed close to the transmitter and equipped with N_1 reflecting elements while RIS 2 is assumed to be placed close to the receiver and equipped with N_2 reflecting elements.

Let $\boldsymbol{H}_\text{T} \in \mathbb{C}^{N_1 \times M_{\text{Tx}}}$, $\boldsymbol{H}_\text{S} \in \mathbb{C}^{N_2 \times N_1}$, and $\boldsymbol{H}_\text{R} \in \mathbb{C}^{M_{\text{Rx}} \times N_2}$ be the transmitter to RIS 1, RIS 1 to RIS 2, and RIS 2 to receiver channels, respectively. We assume that we send L symbols during the training phase. Moreover, L is divided into three transmission blocks as $L = I \cdot J \cdot K$. The received

[1]In this work, we consider deployment scenarios where the other propagation channels, i.e., the transmitter to receiver, the transmitter to RIS 2, and the RIS 1 to receiver channels are neglectable (e.g, in a tunnel) due to severe signal blockage and pathloss. Other scenarios where the aforementioned channels are non negligible are left for future research.

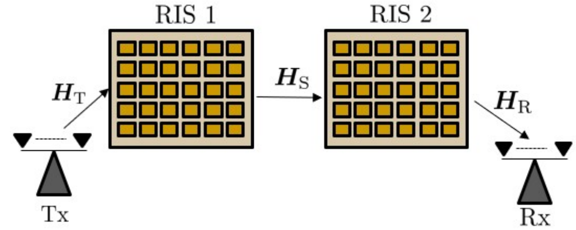

Fig. 1. A D-RIS aided MIMO Communication System

signal at the (j,i,k)th transmission time, $j \in \{1, \cdots, J\}, i \in \{1, \cdots, I\}, k \in \{1, \cdots, K\}$, can be expressed as

$$\bar{\boldsymbol{y}}_{j,i,k} = \boldsymbol{H}_\text{R} \boldsymbol{\Psi}_j \boldsymbol{H}_\text{S} \boldsymbol{\Phi}_i \boldsymbol{H}_\text{T} \boldsymbol{x}_k + \bar{\boldsymbol{n}}_{j,i,k} \in \mathbb{C}^{M_{\text{Rx}}}, \qquad (1)$$

where $\boldsymbol{x}_k \in \mathbb{C}^{M_{\text{Tx}}}$ is the kth training vector at the transmitter with $\|\boldsymbol{x}_j\| = 1$, $\boldsymbol{\Psi}_j = \text{diag}\{\boldsymbol{\psi}_j\}$ is the jth diagonal reflection matrix of RIS 2 with $\boldsymbol{\psi}_j \in \mathbb{C}^{N_2}$ and $|[\boldsymbol{\psi}_j]_{[n_2]}| = 1/\sqrt{N_2}$, $\boldsymbol{\Phi}_i = \text{diag}\{\boldsymbol{\phi}_i\}$ is the ith diagonal reflection matrix of RIS 1, with $\boldsymbol{\phi}_i \in \mathbb{C}^{N_1}$ and $|[\boldsymbol{\phi}_i]_{[n_1]}| = 1/\sqrt{N_1}$, and $\bar{\boldsymbol{n}}_{j,i,j} \in \mathbb{C}^{M_\text{R}}$ is the additive white Gaussian noise vector with zero-mean and variance σ^2.

By stacking the received measurement signals $\{\bar{\boldsymbol{y}}_{j,i,j}, \forall j\}$ next to each other as $\bar{\boldsymbol{Y}}_{j,i} = [\bar{\boldsymbol{y}}_{j,i,1}, \cdots, \bar{\boldsymbol{y}}_{j,i,K}]$, we obtain a measurement matrix $\bar{\boldsymbol{Y}}_{j,i}$ which can be expressed as

$$\bar{\boldsymbol{Y}}_{j,i} = \boldsymbol{H}_\text{R} \boldsymbol{\Psi}_j \boldsymbol{H}_\text{S} \boldsymbol{\Phi}_i \boldsymbol{H}_\text{T} \boldsymbol{X} + \bar{\boldsymbol{N}}_{j,i} \in \mathbb{C}^{M_{\text{Rx}} \times K}, \qquad (2)$$

where $\boldsymbol{X} = [\boldsymbol{x}_1, \cdots, \boldsymbol{x}_K] \in \mathbb{C}^{M_{\text{Tx}} \times K}$ and $\bar{\boldsymbol{N}}_{j,i} \in \mathbb{C}^{M_{\text{Rx}} \times K}$ are defined similarly to $\bar{\boldsymbol{Y}}_{j,i}$. We assume that the training matrix $\boldsymbol{X}$ is designed with orthonormal rows, i.e., $\boldsymbol{X}\boldsymbol{X}^\text{H} = \boldsymbol{I}_{M_{\text{Tx}}}$, which implies that $K \geq M_{\text{Tx}}$. Then, the right filtered measurement matrix $\boldsymbol{Y}_{j,i} = \bar{\boldsymbol{Y}}_{j,i} \boldsymbol{X}^\text{H}$ can be written as

$$\boldsymbol{Y}_{j,i} = \boldsymbol{H}_\text{R} \boldsymbol{\Psi}_j \boldsymbol{H}_\text{S} \boldsymbol{\Phi}_i \boldsymbol{H}_\text{T} + \boldsymbol{N}_{j,i} \in \mathbb{C}^{M_{\text{Rx}} \times M_{\text{Tx}}}, \qquad (3)$$

where $\boldsymbol{N}_{j,i} = \bar{\boldsymbol{N}}_{j,i} \boldsymbol{X}^\text{H}$. Given the measurement matrices in (3), our main goal is to obtain an estimate for the channel matrices $\boldsymbol{H}_\text{T}, \boldsymbol{H}_\text{S}$, and $\boldsymbol{H}_\text{R}$.

III. Proposed Channel Estimation Method

Let $\bar{\boldsymbol{\mathcal{Y}}}_i$ be a 3-way tensor constructed by concatenating the ith block measurement matrices $\boldsymbol{Y}_{1,i}, \boldsymbol{Y}_{2,i}, \ldots, \boldsymbol{Y}_{J,i}$ along the second dimension as

$$\bar{\boldsymbol{\mathcal{Y}}}_i = [\boldsymbol{Y}_{1,i} \sqcup_2 \boldsymbol{Y}_{2,i}, \ldots, \sqcup_2 \boldsymbol{Y}_{J,i}] \in \mathbb{C}^{M_{\text{Rx}} \times J \times M_{\text{Tx}}}, \qquad (4)$$

where $\cup_n$ denotes the concatenation along the nth dimension. Moreover, let $\boldsymbol{\mathcal{Y}}$ be a 4-way tensor constructed by concatenating the measurement tensors $\bar{\boldsymbol{\mathcal{Y}}}_1, \bar{\boldsymbol{\mathcal{Y}}}_2, \ldots, \bar{\boldsymbol{\mathcal{Y}}}_I$ along the forth dimension as

$$\boldsymbol{\mathcal{Y}} = [\bar{\boldsymbol{\mathcal{Y}}}_1 \sqcup_4 \bar{\boldsymbol{\mathcal{Y}}}_2, \ldots, \sqcup_4 \bar{\boldsymbol{\mathcal{Y}}}_I] \in \mathbb{C}^{M_{\text{Rx}} \times J \times M_{\text{Tx}} \times I}. \qquad (5)$$

Here, we observe that the 4-way tensor $\boldsymbol{\mathcal{Y}}$ can be interpreted as a nested PARAFAC decomposition [18], as shown in Fig. 2. Specifically, let $\boldsymbol{\Psi} = [\boldsymbol{\psi}_1, \cdots, \boldsymbol{\psi}_J]^\text{T} \in \mathbb{C}^{J \times N_2}$, $\boldsymbol{\Phi} = [\boldsymbol{\phi}_1, \cdots, \boldsymbol{\phi}_I]^\text{T} \in \mathbb{C}^{I \times N_1}$, and define the following two 3-way PARAFAC tensors $\boldsymbol{\mathcal{A}}$ and $\boldsymbol{\mathcal{B}}$ as

$$\boldsymbol{\mathcal{A}} = \boldsymbol{\mathcal{I}}_{3,N_1} \times_1 \boldsymbol{H}_\text{T}^\text{T} \times_2 \boldsymbol{\Phi} \times_3 \boldsymbol{H}_\text{S} \in \mathbb{C}^{M_{\text{Tx}} \times I \times N_2}, \qquad (6)$$
$$\boldsymbol{\mathcal{B}} = \boldsymbol{\mathcal{I}}_{3,N_2} \times_1 \boldsymbol{H}_\text{R} \times_2 \boldsymbol{\Psi} \times_3 \boldsymbol{H}_\text{S}^\text{T} \in \mathbb{C}^{M_{\text{Rx}} \times J \times N_1}.$$

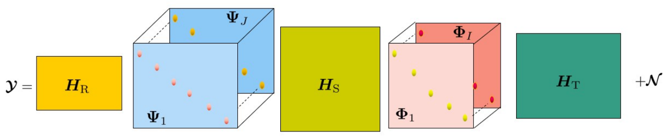

Fig. 2. Graphical representation of the 4-way tensor $\mathcal{Y}$

Algorithm 1 Khatri-Rao Factorization (KRF)

Input: $\boldsymbol{T} \in \mathbb{C}^{P\times Q}$
for $q = 1$ to Q **do**
  Get $\boldsymbol{T}_q = \text{unvec}\{[\boldsymbol{T}]_{[:,q]}\} = [\boldsymbol{R}]_{[:,q]}[\boldsymbol{L}]^{\mathrm{T}}_{[:,q]} \in \mathbb{C}^{P_2\times P_1}$
  Compute SVD of $\boldsymbol{T}_q$ as $\boldsymbol{T}_q = \boldsymbol{u}_q\sigma_q\boldsymbol{v}_q^{\mathrm{H}} \in \mathbb{C}^{P_2\times P_1}$
  Set $[\hat{\boldsymbol{R}}]_{[:,q]} = \sqrt{\sigma_q}\boldsymbol{u}_q$ and $[\hat{\boldsymbol{L}}]_{[:,q]} = \sqrt{\sigma_q}\boldsymbol{v}_q^*$
end for
Output: $\hat{\boldsymbol{L}} \in \mathbb{C}^{P_1\times Q}$ and $\hat{\boldsymbol{R}} \in \mathbb{C}^{P_2\times Q}$

Then, it can be easily shown that the n-mode unfoldings of the 4-way tensor $\mathcal{Y}$, $n = \{1, 2, 3, 4\}$, can be expressed as

$$[\mathcal{Y}]_{(1)} = \boldsymbol{H}_{\mathrm{R}}([\mathcal{A}]^{\mathrm{T}}_{(3)} \diamond \boldsymbol{\Psi})^{\mathrm{T}} + [\mathcal{N}]_{(1)} \in \mathbb{C}^{M_{\mathrm{Rx}}\times IM_{\mathrm{Tx}}J}, \quad (7)$$
$$[\mathcal{Y}]_{(2)} = \boldsymbol{\Psi}([\mathcal{A}]^{\mathrm{T}}_{(3)} \diamond \boldsymbol{H}_{\mathrm{R}})^{\mathrm{T}} + [\mathcal{N}]_{(2)} \in \mathbb{C}^{J\times M_{\mathrm{Rx}}M_{\mathrm{Tx}}I}, \quad (8)$$
$$[\mathcal{Y}]_{(3)} = \boldsymbol{H}_{\mathrm{T}}^{\mathrm{T}}(\boldsymbol{\Phi} \diamond [\mathcal{B}]^{\mathrm{T}}_{(3)})^{\mathrm{T}} + [\mathcal{N}]_{(3)} \in \mathbb{C}^{M_{\mathrm{Tx}}\times IM_{\mathrm{Rx}}J}, \quad (9)$$
$$[\mathcal{Y}]_{(4)} = \boldsymbol{\Phi}(\boldsymbol{H}_{\mathrm{T}}^{\mathrm{T}} \diamond [\mathcal{B}]^{\mathrm{T}}_{(3)})^{\mathrm{T}} + [\mathcal{N}]_{(4)} \in \mathbb{C}^{I\times M_{\mathrm{Rx}}JM_{\mathrm{Tx}}}, \quad (10)$$

where $[\mathcal{A}]_{(3)} = \boldsymbol{H}_{\mathrm{S}}(\boldsymbol{\Phi} \diamond \boldsymbol{H}_{\mathrm{T}}^{\mathrm{T}})^{\mathrm{T}} \in \mathbb{C}^{N_2\times IM_{\mathrm{Tx}}}$ and $[\mathcal{B}]_{(3)} = \boldsymbol{H}_{\mathrm{S}}^{\mathrm{T}}(\boldsymbol{\Psi} \diamond \boldsymbol{H}_{\mathrm{R}})^{\mathrm{T}} \in \mathbb{C}^{N_1\times JM_{\mathrm{Rx}}}$ are the 3-mode unfolding of $\mathcal{A}$ and $\mathcal{B}$, respectively. In the following, we propose two solutions for estimating $\boldsymbol{H}_{\mathrm{T}}$, $\boldsymbol{H}_{\mathrm{S}}$, and $\boldsymbol{H}_{\mathrm{R}}$ by exploiting the above tensor structure.

KRF-based method: Assume that the training matrices $\boldsymbol{\Phi}$ and $\boldsymbol{\Psi}$ are designed with orthonormal columns, i.e., $\boldsymbol{\Phi}^{\mathrm{H}}\boldsymbol{\Phi} = \boldsymbol{I}_I$ and $\boldsymbol{\Psi}^{\mathrm{H}}\boldsymbol{\Psi} = \boldsymbol{I}_J$. Then, the left-filtered 2-mode and 4-mode unfolding matrices are given as

$$[\tilde{\mathcal{Y}}]_{(2)} = \boldsymbol{\Psi}^{\mathrm{H}}[\mathcal{Y}]_{(2)} = ([\mathcal{A}]^{\mathrm{T}}_{(3)} \diamond \boldsymbol{H}_{\mathrm{R}})^{\mathrm{T}} + \boldsymbol{\Psi}^{\mathrm{H}}[\mathcal{N}]_{(2)} \quad (11)$$
$$[\tilde{\mathcal{Y}}]_{(4)} = \boldsymbol{\Phi}^{\mathrm{H}}[\mathcal{Y}]_{(4)} = (\boldsymbol{H}_{\mathrm{T}}^{\mathrm{T}} \diamond [\mathcal{B}]^{\mathrm{T}}_{(3)})^{\mathrm{T}} + \boldsymbol{\Phi}^{\mathrm{H}}[\mathcal{N}]_{(4)}. \quad (12)$$

Given $[\tilde{\mathcal{Y}}]_{(2)}$ and $[\tilde{\mathcal{Y}}]_{(4)}$ as above, the channel matrices $\boldsymbol{H}_{\mathrm{R}}$ and $\boldsymbol{H}_{\mathrm{T}}$ can be estimated as a solution to

$$\hat{\boldsymbol{H}}_{\mathrm{R}} = \text{argmin}_{\boldsymbol{H}_{\mathrm{R}}}\|[\tilde{\mathcal{Y}}]^{\mathrm{T}}_{(2)} - ([\mathcal{A}]^{\mathrm{T}}_{(3)} \diamond \boldsymbol{H}_{\mathrm{R}})\|^2_{\mathrm{F}}, \quad (13)$$
$$\hat{\boldsymbol{H}}_{\mathrm{T}} = \text{argmin}_{\boldsymbol{H}_{\mathrm{T}}}\|[\tilde{\mathcal{Y}}]^{\mathrm{T}}_{(4)} - (\boldsymbol{H}_{\mathrm{T}}^{\mathrm{T}} \diamond [\mathcal{B}]^{\mathrm{T}}_{(3)})\|^2_{\mathrm{F}}. \quad (14)$$

Clearly, both problems have a similar structure given as

$$[\boldsymbol{L}, \boldsymbol{R}] = \text{argmin}_{\boldsymbol{L},\boldsymbol{R}}\|\boldsymbol{T} - (\boldsymbol{L} \diamond \boldsymbol{R})\|^2_{\mathrm{F}}, \quad (15)$$

assuming that $\boldsymbol{T} = (\boldsymbol{L} \diamond \boldsymbol{R}) \in \mathbb{C}^{P\times Q}$, $\boldsymbol{L} \in \mathbb{C}^{P_1\times Q}$, $\boldsymbol{R} \in \mathbb{C}^{P_2\times Q}$, and $P = P_1P_2$. A closed-form solution to (15) can be obtained using the least squares Khatri-Rao Factorization (KRF) technique [19], as summarized in Algorithm 1[2].

On the other hand, to estimate $\boldsymbol{H}_{\mathrm{S}}$, we exploit the observation that each n-mode unfolding $[\mathcal{Y}]_{(n)}$ of the 4-way tensor $\mathcal{Y}$ can be seen as a 1-mode unfolding of a 3-way tensor. For instance, the 3-mode unfolding $[\mathcal{Y}]_{(3)}$ is equal to the 1-mode unfolding of a 3-way tensor $\mathcal{Z} \in \mathbb{C}^{M_{\mathrm{Tx}}\times JM_{\mathrm{Rx}}\times I}$ given as

$$\mathcal{Z} = \mathcal{I}_{3,N_1} \times_1 \boldsymbol{H}_{\mathrm{T}}^{\mathrm{T}} \times_2 [\mathcal{B}]^{\mathrm{T}}_{(3)} \times_3 \boldsymbol{\Phi} + \mathcal{Q}, \quad (16)$$

where $\mathcal{Q} \in \mathbb{C}^{M_{\mathrm{Tx}}\times JM_{\mathrm{Rx}}\times I}$ is the 3-way noise tensor representation of the 4-way noise tensor $\mathcal{N} \in \mathbb{C}^{M_{\mathrm{Rx}}\times J\times M_{\mathrm{Tx}}\times I}$. Clearly, $[\mathcal{Z}]_{(1)} = [\mathcal{Y}]_{(3)}$. The 2-mode unfolding of $\mathcal{Z}$ is given as

$$\begin{aligned}[\mathcal{Z}]_{(2)} &= [\mathcal{B}]^{\mathrm{T}}_{(3)}(\boldsymbol{\Phi} \diamond \boldsymbol{H}_{\mathrm{T}}^{\mathrm{T}})^{\mathrm{T}} \\ &= (\boldsymbol{\Psi} \diamond \boldsymbol{H}_{\mathrm{R}})\boldsymbol{H}_{\mathrm{S}}(\boldsymbol{\Phi} \diamond \boldsymbol{H}_{\mathrm{T}}^{\mathrm{T}})^{\mathrm{T}} \in \mathbb{C}^{JM_{\mathrm{Rx}}\times IM_{\mathrm{Tx}}}. \quad (17)\end{aligned}$$

Let $\boldsymbol{z}_2 = \text{vec}\{[\mathcal{Z}]_{(2)}\} = \boldsymbol{V}_{\mathrm{S}}\boldsymbol{h}_{\mathrm{S}}$, where $\boldsymbol{h}_{\mathrm{S}} = \text{vec}\{\boldsymbol{H}_{\mathrm{S}}\}$ and $\boldsymbol{V}_{\mathrm{S}} = (\boldsymbol{\Phi} \diamond \boldsymbol{H}_{\mathrm{T}}^{\mathrm{T}}) \otimes (\boldsymbol{\Psi} \diamond \boldsymbol{H}_{\mathrm{R}}) \in \mathbb{C}^{IJM_{\mathrm{Tx}}M_{\mathrm{Rx}}\times N_1N_2}$. Then, an estimate of $\boldsymbol{H}_{\mathrm{S}}$ can be obtained as

$$\hat{\boldsymbol{H}}_{\mathrm{S}} = \text{unvec}\big\{\{\boldsymbol{V}_{\mathrm{S}}\}^{+}\boldsymbol{z}_2\big\}. \quad (18)$$

The proposed closed-form KRF-based channel estimation for D-RIS systems is summarized in Algorithm 2.

Algorithm 2 KRF-based for CE in D-RIS Systems

Input: Measurement tensor $\mathcal{Y} \in \mathbb{C}^{M_{\mathrm{Rx}}\times J\times M_{\mathrm{Tx}}\times I}$
Get $\hat{\boldsymbol{H}}_{\mathrm{R}}$ as a solution to (13) via Algorithm 1
Get $\hat{\boldsymbol{H}}_{\mathrm{T}}$ as a solution to (14) via Algorithm 1
Given $\hat{\boldsymbol{H}}_{\mathrm{R}}$ and $\hat{\boldsymbol{H}}_{\mathrm{T}}$, get $\hat{\boldsymbol{H}}_{\mathrm{S}}$ using (18)
Output: $\hat{\boldsymbol{H}}_{\mathrm{R}}$, $\hat{\boldsymbol{H}}_{\mathrm{T}}$, and $\hat{\boldsymbol{H}}_{\mathrm{S}}$

ALS-based method: An ALS-based method can also be used to estimate the channel matrices $\boldsymbol{H}_{\mathrm{R}}, \boldsymbol{H}_{\mathrm{T}}$, and $\boldsymbol{H}_{\mathrm{S}}$. Specifically, given $[\mathcal{Y}]_{(1)}$ and $[\mathcal{Y}]_{(3)}$, an estimate for $\boldsymbol{H}_{\mathrm{R}}$ and $\boldsymbol{H}_{\mathrm{T}}$ can be obtained as

$$\hat{\boldsymbol{H}}_{\mathrm{R}} = [\mathcal{Y}]_{(1)}\big\{([\mathcal{A}]^{\mathrm{T}}_{(3)} \diamond \boldsymbol{\Psi})^{\mathrm{T}}\big\}^{+} = [\mathcal{Y}]_{(1)}\{\boldsymbol{V}_{\mathrm{R}}\}^{+} \quad (19)$$
$$\hat{\boldsymbol{H}}_{\mathrm{T}}^{\mathrm{T}} = [\mathcal{Y}]_{(3)}\big\{(\boldsymbol{\Phi} \diamond [\mathcal{B}]^{\mathrm{T}}_{(3)})^{\mathrm{T}}\big\}^{+} = [\mathcal{Y}]_{(3)}\{\boldsymbol{V}_{\mathrm{T}}\}^{+}, \quad (20)$$

where $\boldsymbol{V}_{\mathrm{R}} = \big((\boldsymbol{\Phi} \diamond \boldsymbol{H}_{\mathrm{T}}^{\mathrm{T}})\boldsymbol{H}_{\mathrm{S}}^{\mathrm{T}} \diamond \boldsymbol{\Psi}\big)^{\mathrm{T}} \in \mathbb{C}^{N_2\times IJM_{\mathrm{Tx}}}$ and $\boldsymbol{V}_{\mathrm{T}} = \big(\boldsymbol{\Phi} \diamond (\boldsymbol{\Psi} \diamond \boldsymbol{H}_{\mathrm{R}})\boldsymbol{H}_{\mathrm{S}}\big)^{\mathrm{T}} \in \mathbb{C}^{N_1\times IJM_{\mathrm{Rx}}}$. Then, using (18), (19), and (20), an ALS-based method can be used to estimate $\boldsymbol{H}_{\mathrm{R}}, \boldsymbol{H}_{\mathrm{T}}$, and $\boldsymbol{H}_{\mathrm{S}}$, respectively, as summarized in Algorithm 3, which is guaranteed to converge monotonically to, at least, a local optimum [20]. However, it is known that the convergence rate of ALS-based methods depends on the initialization, where a good initialization strategy generally leads to a fast convergence rate, and therefore a reduced

Algorithm 3 ALS-based for CE in D-RIS Systems

Input: Measurement tensor $\mathcal{Y} \in \mathbb{C}^{M_{\mathrm{Rx}}\times J\times M_{\mathrm{Tx}}\times I}$
Initialize $\boldsymbol{H}_{\mathrm{R}}^{(0)}$ as solution to (13) and $\boldsymbol{H}_{\mathrm{T}}^{(0)}$ as solution to (14).
Select $L_{\max} \geq 1$
for $\ell = 1$ to $L_{\max}$ **do**
  Given $\boldsymbol{H}_{\mathrm{R}}^{(\ell-1)}$ and $\boldsymbol{H}_{\mathrm{T}}^{(\ell-1)}$, get $\hat{\boldsymbol{H}}_{\mathrm{S}}^{(\ell)}$ using (18)
  Given $\boldsymbol{H}_{\mathrm{T}}^{(\ell-1)}$ and $\boldsymbol{H}_{\mathrm{S}}^{(\ell)}$, get $\hat{\boldsymbol{H}}_{\mathrm{R}}^{(\ell)}$ using (19)
  Given $\boldsymbol{H}_{\mathrm{R}}^{(\ell)}$ and $\boldsymbol{H}_{\mathrm{S}}^{(\ell)}$, get $\hat{\boldsymbol{H}}_{\mathrm{T}}^{(\ell)}$ using (20)
end for
Output: $\hat{\boldsymbol{H}}_{\mathrm{R}}$, $\hat{\boldsymbol{H}}_{\mathrm{T}}$, and $\hat{\boldsymbol{H}}_{\mathrm{S}}$

[2]Note that $\boldsymbol{T}_q \in \mathbb{C}^{P_2\times P_1}$ in Algorithm 1 is a rank-one matrix. Its singular value decomposition (SVD) can be efficiently calculated using the Power Iteration method, which has a low computational complexity.

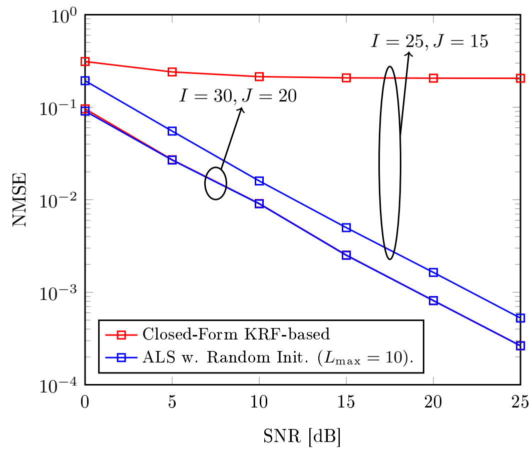

Fig. 3. NMSE versus SNR.

computational complexity. Motivated by the closed-form KRF-based method, we propose to initialize $\boldsymbol{H}_{\mathrm{R}}$ and $\boldsymbol{H}_{\mathrm{T}}$ using (13) and (14), respectively.

Identifiability, in the LS sense, can be obtained by noticing that $\boldsymbol{V}_{\mathrm{R}}$ and $\boldsymbol{V}_{\mathrm{T}}$ must have full column-rank and $\boldsymbol{V}_{\mathrm{S}}$ must have full row-rank. Therefore, Algorithm 3 requires that $IJ \geq \max\left\{\left\lceil \frac{N_2}{M_{\mathrm{Tx}}}\right\rceil, \left\lceil \frac{N_1}{M_{\mathrm{Rx}}}\right\rceil, \left\lceil \frac{N_1 N_2}{M_{\mathrm{Rx}} M_{\mathrm{Tx}}}\right\rceil\right\}$, while its complexity[3] is on the order of $\mathcal{O}\big(L_{\max}\cdot(N_2^3 + N_1^3 + (N_1N_2)^3)\big)$. On the other hand, Algorithm 2 requires that $I \geq N_1$ and $J \geq N_2$, while its complexity is on the order of $\mathcal{O}\big(N_1^2 + N_2^2 + (N_1N_2)^3\big)$. In [14], the ambiguities of the estimated channels were determined under the same assumption for the system model and it was shown that the estimated channels are unique up to scalar ambiguities per column. In particular, these ambiguities between the estimated and the true channels can be written as

$$\hat{\boldsymbol{H}}_{\mathrm{S}} \approx \boldsymbol{\Delta}_{\mathrm{R}}^{-1}\boldsymbol{H}_{\mathrm{S}}\boldsymbol{\Delta}_{\mathrm{T}}^{-1}, \quad \hat{\boldsymbol{H}}_{\mathrm{R}} \approx \boldsymbol{H}_{\mathrm{R}}\boldsymbol{\Delta}_{\mathrm{R}}, \quad \hat{\boldsymbol{H}}_{\mathrm{T}} \approx \boldsymbol{\Delta}_{\mathrm{T}}\boldsymbol{H}_{\mathrm{T}}, \quad (21)$$

where $\boldsymbol{\Delta}_{\mathrm{T}}$ and $\boldsymbol{\Delta}_{\mathrm{R}}$ are diagonal matrices holding the scaling ambiguities. Note that these scalar ambiguities have no impact on the active and passive RIS reflection design of $\boldsymbol{\Phi}$ and $\boldsymbol{\Psi}$. Let $\hat{\boldsymbol{H}}_{\mathrm{cascaded}} = \hat{\boldsymbol{H}}_{\mathrm{R}}\boldsymbol{\Psi}\hat{\boldsymbol{H}}_{\mathrm{S}}\boldsymbol{\Phi}\hat{\boldsymbol{H}}_{\mathrm{T}} \in \mathbb{C}^{M_{\mathrm{Rx}}\times M_{\mathrm{Tx}}}$ be the cascaded channel. Substituting the estimated channels given in (21) in the cascaded channel $\hat{\boldsymbol{H}}_{\mathrm{cascaded}}$, it can be seen that that the diagonal ambiguity matrices $\boldsymbol{\Delta}_{\mathrm{T}}$ and $\boldsymbol{\Delta}_{\mathrm{R}}$ commute and they cancel with their inverses. Therefore, the performance of the system in terms of the spectral efficiency does not depend on the knowledge of each channel $\boldsymbol{H}_{\mathrm{T}}$, $\boldsymbol{H}_{\mathrm{S}}$, and $\boldsymbol{H}_{\mathrm{R}}$ separately but only on the cascaded channel.

IV. Simulation Results

We assume that the entries of the channels $\boldsymbol{H}_{\mathrm{R}}, \boldsymbol{H}_{\mathrm{T}}$, and $\boldsymbol{H}_{\mathrm{S}}$ are independent and identically distributed with zero-mean circularly-symmetric complex Gaussian random variables. The results are shown in terms of the normalized-mean-squared-error (NMSE) of the effective channel defined as $\mathrm{NMSE} = \mathbb{E}\{\|\boldsymbol{H}_{\mathrm{e}} - \hat{\boldsymbol{H}}_{\mathrm{e}}\|_{\mathrm{F}}^2\}/\mathbb{E}\{\|\boldsymbol{H}_{\mathrm{e}}\|_{\mathrm{F}}^2\}$, where $\boldsymbol{H}_{\mathrm{e}} = \boldsymbol{H}_{\mathrm{R}}\boldsymbol{H}_{\mathrm{S}}\boldsymbol{H}_{\mathrm{T}}$ and $\hat{\boldsymbol{H}}_{\mathrm{e}} = \hat{\boldsymbol{H}}_{\mathrm{R}}\hat{\boldsymbol{H}}_{\mathrm{S}}\hat{\boldsymbol{H}}_{\mathrm{T}}$. The signal-to-noise ratio is defined as

[3]Here, we have assumed that the complexity of calculating the Moore-Penrose inverse of a $m \times n$ matrix is on the order of $\mathcal{O}(\min\{n, m\}^3)$.

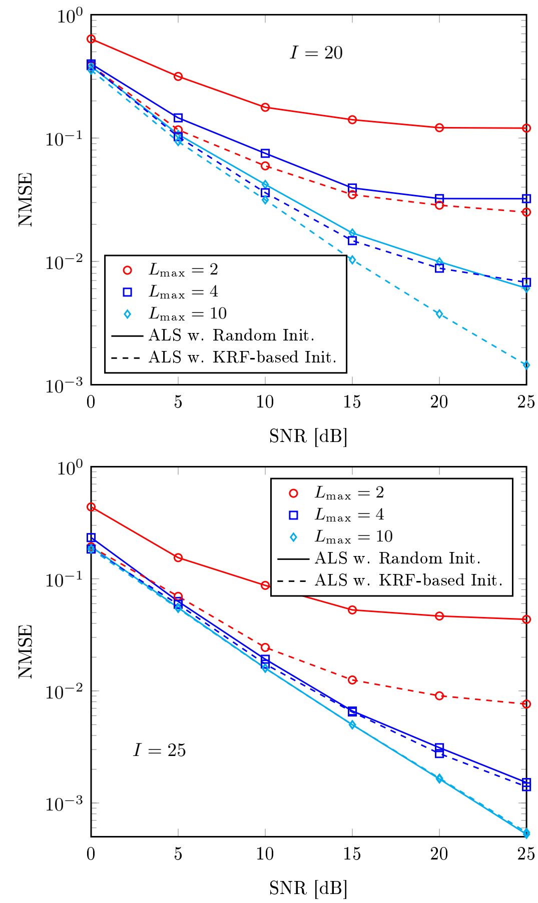

Fig. 4. NMSE vs. SNR. for $J = 15$

$\mathrm{SNR} = \mathbb{E}\{\|\boldsymbol{\mathcal{Y}} - \boldsymbol{\mathcal{N}}\|_{\mathrm{F}}^2\}/\mathbb{E}\{\|\boldsymbol{\mathcal{N}}\|_{\mathrm{F}}^2\}$. Assuming that $I \leq N_1$ and $J \leq N_2$, the training matrices $\boldsymbol{\Phi} \in \mathbb{C}^{I\times N_1}$ and $\boldsymbol{\Psi} \in \mathbb{C}^{J\times N_2}$ are designed by randomly selecting I and J rows from normalized N_1-DFT and N_2-DFT matrices, respectively. In all simulation results, we assume that $M_{\mathrm{Tx}} = 2$, $M_{\mathrm{Rx}} = 4$, $N_1 = 30$, $N_2 = 20$, and $K = M_{\mathrm{T}}$.

In Fig. 3, we show the NMSE versus the SNR results comparing the two proposed channel estimation methods, the closed-form KRF-based method, i.e., Algorithm 2 and the ALS-based method, i.e., Algorithm 3. From Fig. 3, we can see that when I and J are selected such that $I = N_1$ and $J = N_2$, both methods achieve the best performance. However, the estimation accuracy of Algorithm 2 degrades significantly if $I < N_1$ and $J < N_2$, since the identifiability constraints for closed-form KRF are not satisfied. However, Algorithm 3 can still achieve a good performance only after $L_{\max} = 10$ iterations, at the expense of a higher complexity.

In Fig. 4, we show the NMSE versus the SNR results comparing the proposed ALS-based method with KRF-based initialization, i.e., Algorithm 3 and the ALS-based method with random initialization proposed in [14]. As it can be seen, Algorithm 3 not only enjoys a faster convergence rate as compared to the ALS-based method with random initialization, but also achieves a better channel estimation accuracy, especially with a low training overhead. If we assume that the transmitter in this work represents a base station in a practical scenario, then the required training overhead can be further reduced. The reason is that due to the fixed position of the base station, RIS 1, and RIS 2, $\boldsymbol{H}_\mathrm{T}$ and $\boldsymbol{H}_\mathrm{S}$ are slowly fading channel matrices, which do not need to be estimated frequently. Since the aforementioned observation is not exploited in this work, the provided results can be seen as the worst-case, i.e., upper-bound, of the channel estimation accuracy.

V. Conclusions

In this work, we propose a generalized channel estimation technique for D-RIS aided MIMO systems where the training overhead for each RIS can be selected separately. We have shown that an accurate channel estimation can be obtained with a small training overhead by capitalizing on the nested PARAFAC model of the received training signal. Our results show that we can achieve a good performance with ALS-based channel estimation especially in scenarios with small training overhead by using the closed-form KRF method as an initialization strategy.

References

[1] C. Liaskos, S. Nie, A. Tsioliaridou, A. Pitsillides, S. Ioannidis and I. Akyildiz, "A New Wireless Communication Paradigm through Software-Controlled Metasurfaces," IEEE Communications Magazine, vol. 56, no. 9, pp. 162-169, Sept. 2018, doi: 10.1109/MCOM.2018.1700659.

[2] C. Huang, A. Zappone, G. C. Alexandropoulos, M. Debbah and C. Yuen, "Reconfigurable Intelligent Surfaces for Energy Efficiency in Wireless Communication," IEEE Transactions on Wireless Communications, vol. 18, no. 8, pp. 4157-4170, Aug. 2019, doi: 10.1109/TWC.2019.2922609.

[3] S. Zhang and R. Zhang, "Capacity Characterization for Intelligent Reflecting Surface Aided MIMO Communication," IEEE Journal on Selected Areas in Communications, vol. 38, no. 8, pp. 1823-1838, Aug. 2020, doi: 10.1109/JSAC.2020.3000814.

[4] S. Gherekhloo, K. Ardah, A. L. F. de Almeida and M. Haardt, "Tensor-Based Channel Estimation and Reflection Design for RIS-Aided Millimeter-Wave MIMO Communication Systems," in Proc. 55th Asilomar Conference on Signals, Systems, and Computers, Pacific Grove, CA, USA, 2021, pp. 1683-1689, doi: 10.1109/IEEECONF53345.2021.9723362.

[5] K. Ardah, S. Gherekhloo, A. L. F. de Almeida and M. Haardt, "TRICE: A Channel Estimation Framework for RIS-Aided Millimeter-Wave MIMO Systems," IEEE Signal Processing Letters, vol. 28, pp. 513-517, 2021, doi: 10.1109/LSP.2021.3059363.

[6] J. Chen, Y. -C. Liang, Y. Pei and H. Guo, "Intelligent Reflecting Surface: A Programmable Wireless Environment for Physical Layer Security," IEEE Access, vol. 7, pp. 82599-82612, 2019, doi: 10.1109/ACCESS.2019.2924034.

[7] E. Björnson and L. Sanguinetti, "Power Scaling Laws and Near-Field Behaviors of Massive MIMO and Intelligent Reflecting Surfaces," IEEE Open Journal of the Communications Society, vol. 1, pp. 1306-1324, 2020, doi: 10.1109/OJCOMS.2020.3020925.

[8] J. Zhang, C. Qi, P. Li and P. Lu, "Channel Estimation for Reconfigurable Intelligent Surface Aided Massive MIMO System," in Proc. IEEE 21st International Workshop on Signal Processing Advances in Wireless Communications (SPAWC), Atlanta, GA, USA, 2020, pp. 1-5, doi: 10.1109/SPAWC48557.2020.9154276.

[9] H. Guo, Y. -C. Liang, J. Chen and E. G. Larsson, "Weighted Sum-Rate Maximization for Reconfigurable Intelligent Surface Aided Wireless Networks," IEEE Transactions on Wireless Communications, vol. 19, no. 5, pp. 3064-3076, May 2020, doi: 10.1109/TWC.2020.2970061.

[10] S. Guo, Y. Hou, J. Mao, N. Li, H. Chen and X. Tao, "Double RIS-based Hybrid Beamforming Design for MU-MISO mmWave Communication Systems," in Proc. IEEE/CIC International Conference on Communications in China (ICCC), Sanshui, Foshan, China, 2022, pp. 220-225.

[11] Y. Han, S. Zhang, L. Duan and R. Zhang, "Cooperative Double-IRS Aided Communication: Beamforming Design and Power Scaling," IEEE Wireless Communications Letters, vol. 9, no. 8, pp. 1206-1210, Aug. 2020, doi: 10.1109/LWC.2020.2986290.

[12] C. You, B. Zheng and R. Zhang, "Wireless Communication via Double IRS: Channel Estimation and Passive Beamforming Designs," IEEE Wireless Communications Letters, vol. 10, no. 2, pp. 431-435, Feb. 2021.

[13] B. Zheng, C. You and R. Zhang, "Efficient Channel Estimation for Double-IRS Aided Multi-User MIMO System," IEEE Transactions on Communications, vol. 69, no. 6, pp. 3818-3832, June 2021.

[14] K. Ardah, S. Gherekhloo, A. L. F. de Almeida and M. Haardt, "Double-RIS Versus Single-RIS Aided Systems: Tensor-Based MIMO Channel Estimation and Design Perspectives," ICASSP 2022 - in Proc. IEEE International Conference on Acoustics, Speech and Signal Processing (ICASSP), Singapore, Singapore, 2022, pp. 5183-5187, doi: 10.1109/ICASSP43922.2022.9746287.

[15] G. T. de Araújo, A. L. F. de Almeida and R. Boyer, "Channel Estimation for Intelligent Reflecting Surface Assisted MIMO Systems: A Tensor Modeling Approach," IEEE Journal of Selected Topics in Signal Processing, vol. 15, no. 3, pp. 789-802, April 2021, doi: 10.1109/JSTSP.2021.3061274.

[16] G. T. de Araújo and A. L. F. de Almeida, "PARAFAC-Based Channel Estimation for Intelligent Reflective Surface Assisted MIMO System," in Proc. IEEE 11th Sensor Array and Multichannel Signal Processing Workshop (SAM), Hangzhou, China, 2020, pp. 1-5, doi: 10.1109/SAM48682.2020.9104260.

[17] G. T. de Araújo, A. L. F. de Almeida and R. Boyer, "Channel Estimation for Intelligent Reflecting Surface Assisted MIMO Systems: A Tensor Modeling Approach," IEEE Journal of Selected Topics in Signal Processing, vol. 15, no. 3, pp. 789-802, April 2021, doi: 10.1109/JSTSP.2021.3061274.

[18] A. L. F. de Almeida and G. Favier, "Double Khatri–Rao Space-Time-Frequency Coding Using Semi-Blind PARAFAC Based Receiver," IEEE Signal Processing Letters, vol. 20, no. 5, pp. 471-474, May 2013, doi: 10.1109/LSP.2013.2248149.

[19] L. R. Ximenes, G. Favier and A. L. F. de Almeida, "Closed-Form Semi-Blind Receiver For MIMO Relay Systems Using Double Khatri–Rao Space-Time Coding," IEEE Signal Processing Letters, vol. 23, no. 3, pp. 316-320, March 2016, doi: 10.1109/LSP.2016.2518699.

[20] Comon, P., Luciani, X. and de Almeida, A.L.F., Tensor decompositions, alternating least squares and other tales. J. Chemometrics, 23: 393-405, 2009, https://doi.org/10.1002/cem.1236.

[21] F. Roemer and M. Haardt, "Tensor-based channel estimation (TENCE) for two-way relaying with multiple antennas and spatial reuse," in Proc. IEEE International Conference on Acoustics, Speech and Signal Processing, Taipei, Taiwan, 2009, pp. 3641-3644, doi: 10.1109/ICASSP.2009.4960415.